J Electroceram (2011) 27:78–82
DOI 10.1007/s10832-011-9652-9

Preparation and properties of strontium barium niobate based glass-ceramics for energy storage capacitors

Guo-hua Chen · Wen-jun Zhang · Xin-yu Liu · Chang-rong Zhou

Received: 30 September 2010 / Accepted: 24 August 2011 / Published online: 1 September 2011

Abstract Na_2O–BaO–SrO–Nb_2O_5–B_2O_3–SiO_2 glass-ceramics were prepared by melt-casting followed by controlled crystallization. X-ray diffraction results show that $Ba_{0.27}Sr_{0.75}Nb_2O_{5.78}$ with tungsten bronze structure formed as the dielectric phases from the glass matrix at 800°C. However, a secondary phase $NaSr_{1.2}Ba_{0.8}Nb_5O_{15}$ occurs when crystallization temperature exceeds 850°C. The glass-ceramics exhibit excellent stability in permittivity values from room temperature to 200°C and low dielectric losses below 0.05. Electrical testing demonstrates that the breakdown strength increases with crystallization temperature. The *P–E* characteristics at room temperature do not show any clear ferroelectric behavior. The glass-ceramic material heated at 800°C/3 h+950°C/3 h shows a breakdown strength of 1400 kV/cm and its energy storage density can reach up to 4.0 J/cm^3, which may be a strong candidate for high energy density storage capacitors for portable or pulsed power applications.

Keywords Glass-ceramics · Strontium barium niobate · Electrical property · Capacitor

G.-h. Chen (✉) · W.-j. Zhang · X.-y. Liu · C.-r. Zhou
School of Materials Science and Engineering,
Guilin University of Electronic Technology,
Guilin 541004, China
e-mail: cgh1682002@163.com

G.-h. Chen
e-mail: chengh@guet.edu.cn

G.-h. Chen · X.-y. Liu · C.-r. Zhou
Guangxi Key Laboratory of Information Materials,
Guilin University of Electronic Technology,
Guilin 541004, China

1 Introduction

In recent years there has been increased research on high energy density storage capacitors for portable/pulsed power applications [1, 2]. For linear dielectric materials, the volumetric energy density is given by [3]:

$$W = \varepsilon_0 \varepsilon_1 E^2/2 \quad (1)$$

Where W is energy storage density (J/cm^3), ε_0 is the vacuum permittivity (8.85×10^{-14} F/cm), ε_r is the relative permittivity and E is the applied electrical field (kV). The above equation shows energy density can be improved by increasing ε_r and/or electrical breakdown strength.

In practice, different types of materials have been explored for high energy density storage capacitors. Polymers are commonly used for such applications, mainly due to their high breakdown strength (>5 MV/cm) despite relatively low ε_r (<5) [4]. Glass materials also offer high breakdown strength but relatively low ε_r [5]. There have been attempts to increase ε_r while maintaining high breakdown strength. Ceramics (such as $BaTiO_3$ and Pb$(Zr_{1-x}Ti_x)$ O_3 with perovskite structure) generally exhibit higher ε_r as compared to polymer and glass materials. The breakdown strength, however, generally decreases with increasing ε_r. Another common approach is to develop composites based on glass-ceramics [6, 7] or polymer-ceramics [8] with the potential to get high ε_r (associated with ceramics) and breakdown strength (associated with glass/polymers) simultaneously. Advantages of using glass-ceramics also include easy adjustability of composition and microstructure, and consequently good tunability of dielectric properties through changing glass composition before melt-casting and subsequent post-treatments.

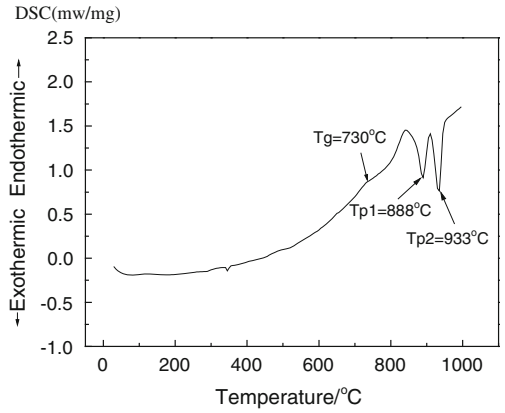

Fig. 1 DSC curve of the as-annealed glass powder at a heating rate of 10 K/min

$Sr_{1-x}Ba_xNb_2O_6$ (SBN) is a well known lead-free relaxor ferroelectric material with a tetragonal tungsten bronze (TTB) structure. SBN accommodates a wide range of Sr/Ba ratio and therefore exhibit variable dielectric properties depending on composition [9]. A few glass-ceramics systems based on SBN have been reported [10, 11].

In this work, we focus on the fabrication of glass-ceramics in the new lead-free glass system of Na_2O–BaO–SrO–Nb_2O_5–B_2O_3–SiO_2 with SBN as the main crystalline dielectric phase. The influences of heat treatment procedure on crystallization, microstructure, dielectric properties, *P–E* hysteresis loops and energy storage density were investigated.

2 Experimental

$5Na_2O$–$20.8BaO$–$20.8SrO$–$18.4Nb_2O_5$–$30SiO_2$–$5B_2O_3$(mol%)glass was prepared using high purity $BaCO_3$(99.5%), $SrCO_3$(99.5%), $NaCO_3$(99.5%), Nb_2O_5(99.5%), H_3BO_3(99.5%) and SiO_2(99.0%). Well-mixed powder mixtures were melted in an alumina crucible at 1530°C for 2 h, and then quickly removed from the

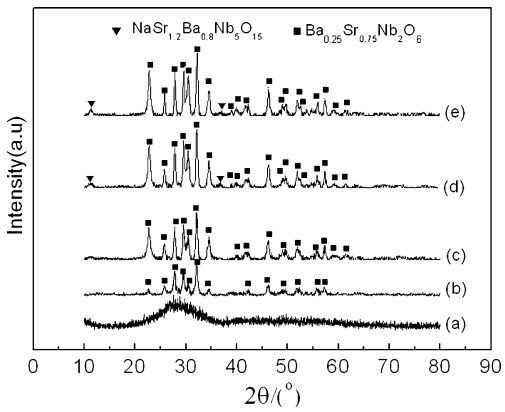

Fig. 2 XRD patterns of the heated glass-ceramics: (a) as-annealed glass; (b) 800°C/3 h; (c) 800°C/3 h+850°C/3 h; (d) 800°C/3 h+900°C/3 h; (e) 800°C/3 h+950°C/3 h

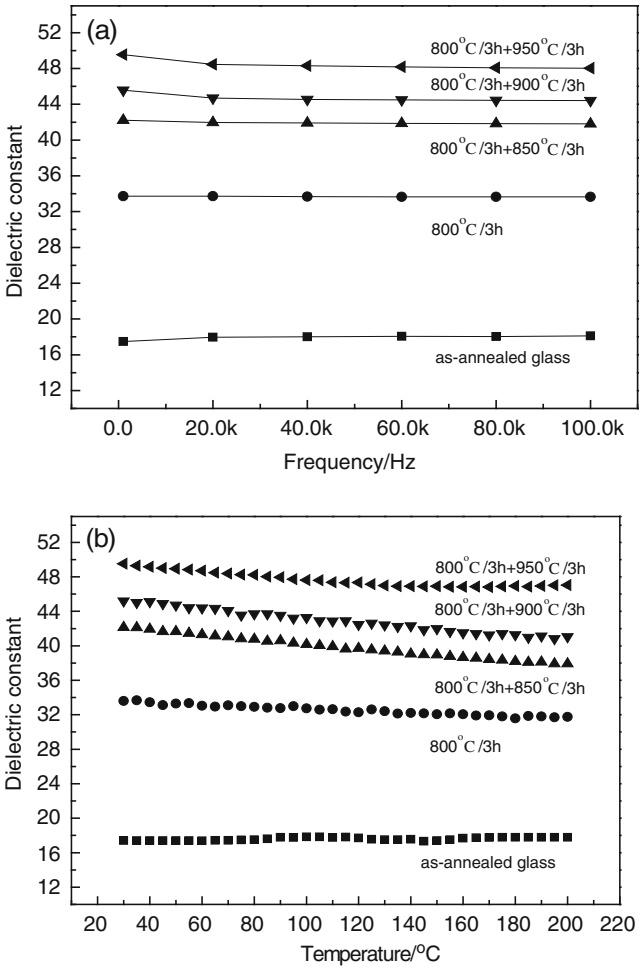

Fig. 3 (a) Frequency dependence of dielectric constant, (b) temperature dependence of dielectric constant for the samples at different heat treatment procedure at 1 kHz

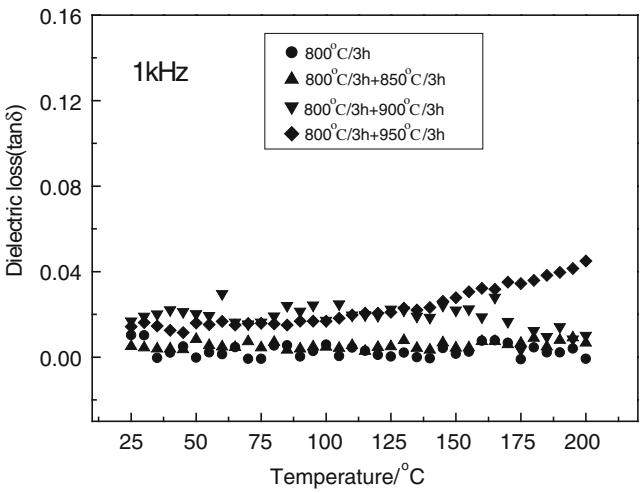

Fig. 4 Dielectric losses as a function of testing temperature for the samples at different crystallization conditions

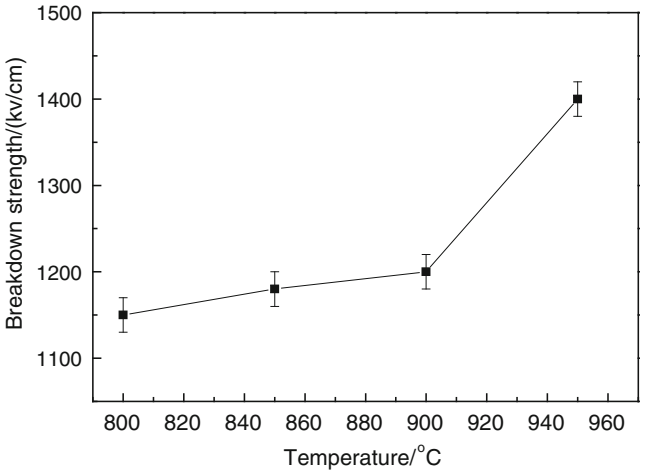

Fig. 5 Breakdown strength of the glass-ceramic samples at different crystallization temperature

furnace, poured onto pre-heated copper plate and pressed to form glass sheets with thickness~1 mm. Next, the glass sheets were immediately annealed at 600°C for 10 h to eliminate internal stress and then furnace-cooled to room temperature. Glass-ceramics were formed by heat treating these glasses in air at specified temperature range.

Differential scanning calorimetry (DSC) measurements (Model STA-449-F3-Jupiter, Netzsch) were carried out by heating approximately 0.5 g of glass powder in a Pt crucible to 1000°C at a heating rate of 10 K/min in flowing air. The glasses were heat-treated under different conditions according to nucleation and crystallization temperature identified by DSC. The developed phases were examined using X-ray Diffractometer (XRD, Model D8-Advance, Bruker) operated at 35 kV/30 mA. The samples were scanned at 1°/min over the 2θ range from 10–80°. Microstructure of the samples was examined by a Scanning Electron Microscope (SEM, Model JSM 5610LV, JEOL). Dielectric properties were tested by a precision multifunction LCR meter (Model HP4292A, Agilent) in the temperature range of 25–200°C and frequency range of 100 Hz–100 kHz. Gold electrodes were sputtered on both sides of the glass-ceramic sheets prior to measurements. The circular samples 10 mm in diameter and 0.4–0.5 mm were prepared for breakdown strength testing. Breakdown strength was performed at room temperature by a home-made clamp which was fully immersed in silicone oil to avoid electric breakdown of the air under high voltage, which was provided by a high-voltage source (Model MARX, Tianjin Dongwen Company, China). Twelve samples for each heat treatment procedure were measured to obtain the average breakdown strength. The breakdown voltage was indicated by the large current impulse generated in the circuit upon sample breakdown (tripping a circuit breaker), and corroborated by the strong visible light emission, audible discharge, and visible surface damage accompanying failure. The *P–E* hysteresis loops were measured by using a ferroelectric tester (Precision Premier II, USA) at room temperature and at 100 Hz.

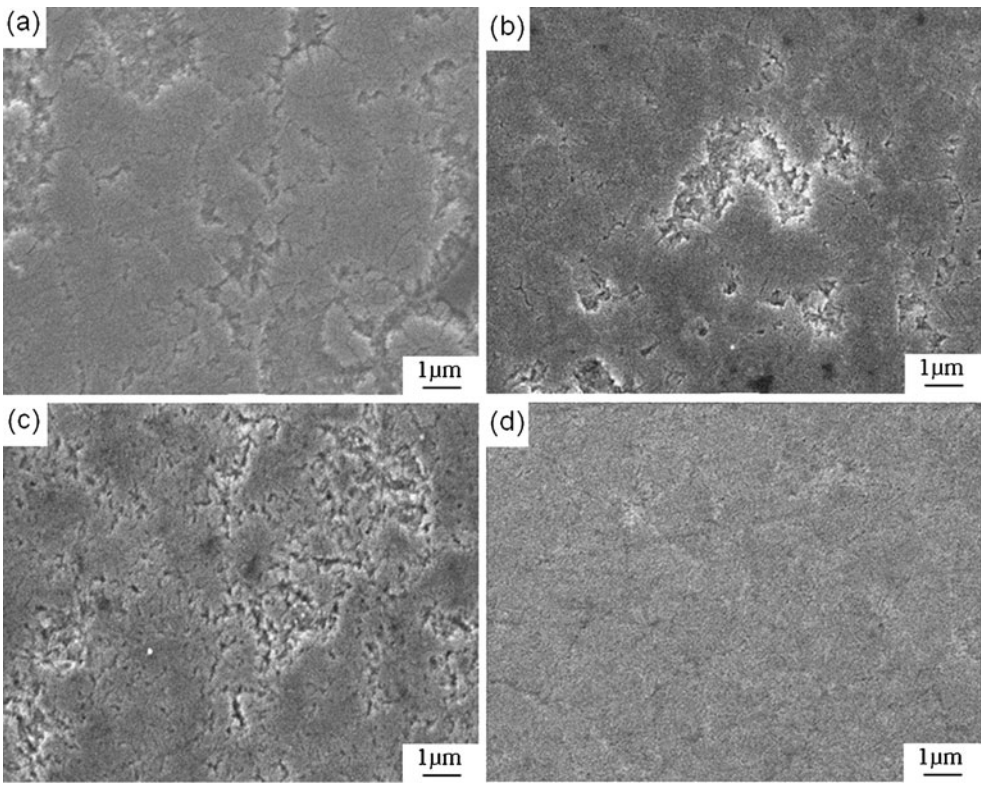

Fig. 6 SEM images of the etched surface of glass-ceramics at different heat treatment procedure: (a)800°C/3 h, (b)800°C/3 h+850°C/3 h, (c)800°C/3 h+900°C/3 h, and (d) 800°C/3 h+950°C/3 h

3 Results and discussion

3.1 DSC analysis

A DSC curve of the as-annealed glass is shown in Fig. 1. It is observed that an endothermic dip at about 730°C, normally called as glass transition temperature, appears in the DSC curve, which is attributed to the transition of the glass structure. With further increase of temperature, two exothermic peaks, *T*p1 and *T*p2, which is related to the crystallization of dielectric phases from glass matrix, are observed with maximum intensity located at 888°C and 933°C, respectively. Therefore, the reasonable nucleation temperature selected is 800°C and the crystallization temperature is in the range of 850–950°C. The glass samples are crystallized by two-stage heat treatment procedure (800°C /3 h+(850–950°C /3 h). The heating rate is 5 K/ min.

3.2 XRD analysis

Evolution of phases during heat-treatment is tracked by XRD analysis, as shown in Fig. 2. The as-annealed glass shows a broad peak, which is indicative of its amorphous nature. XRD pattern for the glass, heat treated at 800°C, shows the presence of $Ba_{0.25}Sr_{0.75}Nb_2O_6$ with tungsten bronze structure (Fig. 2b). This phase continues to grow with increasing temperature (Fig. 2c), which is consistent with the first exothermal peak in the DSC curve that appears at 888°C. On further crystallization at 900°C, the main phase is still $Ba_{0.25}Sr_{0.75}Nb_2O_6$. However, a secondary phase $NaSr_{1.2}Ba_{0.8}Nb_5O_{15}$ comes out. $Ba_{0.25}Sr_{0.75}Nb_2O_6$ and $NaSr_{1.2}Ba_{0.8}Nb_5O_{15}$ co-exist at 950°C. It is evident that two phases appear to grow with increasing temperature, as shown in Fig. 2(d) and (e).

3.3 Dielectric behavior

The dielectric constants of the heated glass-ceramics tested at room temperature from 100 Hz~100 kHz are shown in Fig. 3(a). The dielectric constant of as-annealed glass is 17.5. It is apparent that the dielectric constants increase with crystallization temperature due to the formation of dielectric phases. The dielectric constant obviously increases from 800°C to 850°C, which is mainly due to the formation of high permittivity $Ba_{0.25}Sr_{0.75}Nb_2O_6$ ($\varepsilon_r \approx 1150$) phase [9]. When the crystallization temperature is more than 850°C, the persistent increase of dielectric constant may be ascribed to the increase of dielectric phase contents of $Ba_{0.25}Sr_{0.75}Nb_2O_6$ and $NaSr_{1.2}Ba_{0.8}Nb_5O_{15}$ ($\varepsilon_r \approx 240$) [12], as shown in Fig. 2. From Fig. 3(a), it is also indicated that the dielectric constant of each sample keeps steady over frequency range 100 Hz to 100 kHz. The difference of the dielectric constant value is less than 6% at this frequency range.

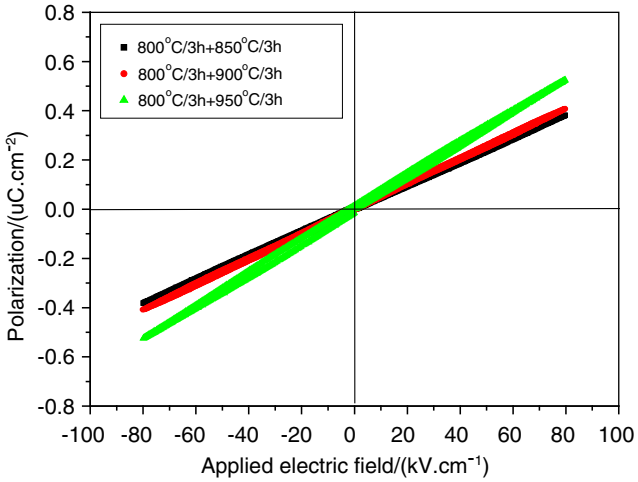

Fig. 7 Room temperature polarization versus electric field data on the glass-ceramics

Figure 3(b) shows the dielectric constant of the sample s as a function of testing temperature. The dielectric constant of as-annealed glass almost keeps constant at this testing temperature range. While the crystallization temperature is increased to 800–900°C, the dielectric constant slightly reduces with the increase of testing temperature, which may be attributed to low amount of $Ba_{0.27}Sr_{0.75}Nb_2O_{5.78}$ phase with Curie temperature of ~60°C [9]. At 950°C, the dielectric constant firstly decreases and then keeps steady with testing temperature. On the whole, all the glass-ceramics show excellent stability in permittivity values from room temperature to 200°C.

Figure 4 shows the dielectric loss of the samples as a function of testing temperature at different heat treatment procedure. The dielectric loss heated at 800°C almost keeps constant in this testing temperature range because there is the lowest amount of dielectric phase occurred in the material. When sample is heat treated at 800°C, 850°C and 900°C, the dielectric loss slightly increases with the increase of testing temperature. This trend may be attributed to relative high amount of dielectric phase. It is noted that dielectric loss of the glass-ceramic heated at

Table 1 Energy storage density of the as-prepared glass-ceramics

Heat treatment procedure	Energy storage density /(J/cm^3)
800°C/3 h	2.0
800°C /3 h+850°C /3 h	2.6
800°C /3 h+900°C /3 h	2.8
800°C /3 h+950°C /3 h	4.0

950°C distinctly increases for high temperature(>150°C), which may be due to the formation of ferroelectric phase $Sr_{1.2}Ba_{0.8}NaNb_5O_{15}$ and conductive processes involving perhaps, space-charge or interfacial polarization effects [13]. In a word, all of the glass-ceramics have low dielectric losses below 0.05 at this testing temperature range.

3.4 Breakdown strength

Figure 5 shows the average breakdown strength as a function of crystallization temperature. The breakdown strength increases with crystallization temperature and the maximum value is 1400 kV/cm for the sample heat treated at 950°C. Figure 6 presents the etched surface morphology of as-heated glass-ceramic samples. An average size of the crystallites is of the order of 100–250 nm for all samples. With increasing crystallization temperature, the content of residual glass phase decreases and that of crystalline phase increases. Figure 6(d) shows full dense microstructure of the glass-ceramic sample heated at 800°C /3 h+950°C/3 h as compared to other heat treatment conditions. It is apparent that there exists a good connectivity between the crystallites. In general, the breakdown strength depends on several factors, including porosity, grain size, and extrinsic measurement conditions such as sample thickness, sample area, and electrode configuration [6, 14, 15]. Based on the above analysis, it is suggested that the improvement of breakdown strength is primarily due to the reduction of grain size and pore size, and the decrease of porosity.

3.5 *P–E* hysteresis loops and energy density

Figure 7 shows the polarization–electric field (P–E) hysteresis loops of the as-heated samples, which are measured at 100 Hz and at room temperature. Considering the current status of a ferroelectric tester, the applied electric field amplitude is in the range of −80~80 kV/cm The P–E loops show a gradual increase with increasing crystallization temperature, which is agreement with the dielectric constant, as shown in Fig. 3(a). From Fig. 7, it is apparent that the *P–E* characteristics do not show any clear ferroelectric behavior. Hence, the glass-ceramics can be regarded as a linear dielectric material. It is expected that the theoretical energy storage density can be evaluated using the formula 1, and the results are shown in Table 1. Table 1 shows that the energy storage density increases with the increase of crystallization temperature, which can be easily explained according to the formula 1 mentioned above. The glass-ceramic sample heated at 800°C /3 h+ 950°C /3 h has a high permittivity (~ 50) and breakdown strength (1400 KV/cm), which has been attributed to a summation of factors including highly polarizable ions enhancing the real part of complex permittivity, the low loss and the substantially defect-free quality of the glass-ceramics. Hence, the glass-ceramic sample heated at 800°C /3 h+950°C /3 h has high energy storage density (4.0 J/cm^3), indicating high potential for energy storage and power compression devices.

4 Conclusion

Na_2O–BaO–SrO–Nb_2O_5–B_2O_3–SiO_2 glass-ceramics were prepared by rapid quenching and controlled crystallization process. Remarkably high DC dielectric breakdown strength (1400 kV/cm) and reasonably high permittivity (~ 50) in the glass-ceramics were measured, equating to high energy densities of 4.0 J/cm^3. To our knowledge, this is the first report of such high breakdown strengths in a bulk strontium barium niobate based glass-ceramics. These findings indicate that lead-free multi-component strontium barium niobate glass may be strong candidates for use in high energy density storage capacitors for portable or pulsed power applications.

Acknowledgments This work was supported by the Research funds of The Guangxi Key Laboratory of Information Materials under the Contract No.0710908-01-Z. This work was also supported by Natural Science Foundation of China (NSFC no.51162002)

References

1. B.J. Chu, X. Zhou, K.L. Ren, B. Neese, M. Lin, Q. Wang, F. Bauer, Q.M. Zhang, Science **313**(5785), 334–336 (2006)
2. E.P. Gorzkowski, M.J. Pan, B. Bender, C.C.M. Wu, J. Electroceram. **18**(3–4), 269–276 (2007)
3. I. Burn, D.M. Smyth, J. Mater. Sci. **7**, 339–343 (1972)
4. J. Li, P. Khanchaitit, K. Han, Q. Wang, Chem. Mater. **22**(18), 5350–5357 (2010)
5. N.J. Test, Mater. Lett. **63**, 1245–1248 (2009)
6. J. Luo, Du Jun, Q. Tang, C. Mao, IEEE Trans. Electron. Dev. **55** (12), 3549–3554 (2008)
7. C.T. Cheng, M. Lanagan, J.T. Lin, B. Jones, M.J. Pan, J. Mater. Res. **20**(2), 438–446 (2005)
8. Y. Bai, Z.-Y. Cheng, V. Bharti, H.S. Xu, Q.M. Zhang, Appl. Phys. Lett. **76**(25), 3804–3806 (2000)
9. Y.-Q. Qu, A.-D. Li, Q.-Y. Shao, Y.-F. Tang, D. Wu, C.L. Mak, K.H. Wong, N.-B. Ming, Mater. Res. Bull. **37**, 503–513 (2002)
10. J.-J. Shyu, C.-H. Chen, Ceram. Int. **29**, 447–453 (2003)
11. J.-J. Shyu, J.-R. Wang, J. Am. Ceram. Soc. **83**(12), 3135–3140 (2000)
12. K. Sambasiva Rao, K.H. Yoon, J. Mater. Sci. **38**, 391–400 (2003)
13. J. Perez, H. Amorin, J.C. M'Peko, J. Portelles, J.A. Perez, F. Guerrero, Mater. Sci. Eng. B **126**(1), 22–27 (2006)
14. T. Tunkasiri, G. Rujijanagul, J. Mater. Sci. Lett. **15**(20), 1767–1769 (1996)
15. E.K. Beauchamp, J. Am. Ceram. Soc **54**(10), 484–1487 (1971)